

Conservation agriculture augments water uptake in wheat: Evidence from modelling**

Surajit Mondal¹, Debashis Chakraborty²^{*}, Pramila Aggarwal², and Tapas K. Das³

¹Division of Crop Research, ICAR Research Complex For Eastern Region, ICAR Parisar, Patna, Bihar, 800014, India

²Division of Agricultural Physics and ³Division of Agronomy, ICAR-Indian Agricultural Research Institute, New Delhi, 110012, India

Received June 26, 2022; accepted November 22, 2022

Abstract. Field water balance and root water uptake in wheat were simulated with Hydrus-2D after a 7-year transition to conservation agriculture. The zero-tilled system with a 40% anchored residue improved soil structure and porosity. Water retention was augmented for most of the growing period, especially in the subsurface (15-30 cm), which was essentially a compact layer (penetration resistance >2500 kPa). The lower soil strength allowed the roots to extend further as compared to conventional tillage. The loss in drainage was reduced by 54-74% over the season using zero tillage with residue. Improved initial crop establishment led to a higher leaf area index and also to an enhanced interception of photosynthetically active radiation. Soil evaporation was also reduced, and root water uptake was 14-17% higher in zero tillage with residue. The grain yield was 17% higher in zero tillage with residue with a marginally higher crop water uptake efficiency. The adoption of conservation agriculture optimized water uptake in wheat by the improving physical condition of the soil and plant water availability. Hydrus-2D was used to successfully simulate the soil water balance and root water uptake in wheat under conservation agriculture. Conservation agriculture requires a redesign of irrigation scheduling, unlike in conventional practice. The simulation of water balance in the soil will aid in irrigation water management in the wheat crop in order to achieve a higher degree of efficiency under conservation agriculture.

Key words: zero tillage, Hydrus-2D, soil water, root uptake, wheat

INTRODUCTION

Conservation agriculture (CA) emphasizes minimum soil disturbance and year-round soil cover by retaining crop residue as mulch or growing cover crops, and also the diversification of the cropping systems (FAO, 2015). CA may contribute to sustainable intensification in South Asia (Jat *et al.*, 2020) and significantly improve the physical condition of the soil in the rice-wheat system (Mondal *et al.*, 2019a, 2020a; Das *et al.*, 2016). Under CA, puddling in rice is avoided, which reduces subsurface compaction and helps to augment root growth in wheat (*e.g.*, Mondal *et al.*, 2019b, 2020a,b; Kukal and Aggarwal, 2003; Whalley *et al.*, 2008). The residue increases the number of retention pores (Mondal *et al.*, 2020a; Jatav *et al.*, 2018), facilitating the water availability to crops under the CA.

A knowledge of soil water dynamics is of fundamental importance for successful crop production, while soil water modelling can be used to optimize management options (Roger-Estrade *et al.*, 2009). Numerical simulations are efficient methods for quantifying the uptake and dynamics of soil water for establishing efficient water management practices (Aggarwal *et al.*, 2017). This necessitates descriptions of soil hydraulic parameters, *i.e.*, soil water content (θ) and hydraulic conductivity as a function of soil water potential [K(h)]. Hydrus-2D (Šimůnek *et al.*, 2008) is

*Corresponding authors e-mail: debashisiari@gmail.com

**The work was partially funded by the Institute project (CRSCI-ARISILZ014025257, 2014-2021) and partially by the PG School, IARI.

a well-accepted process-based model that simulates water movement in the root zone by solving the Richards equation of unsaturated water flow in the soil.

Although CA is being advocated as a better practice in terms of environmental protection and resource utilization than conventional or traditional farmers' practices, limited information is available concerning the soil water balance and root water uptake under CA. The soil matrix and pore system undergoes modification during crop growth, thereby bringing about changes in the soil water system. A simulation of this highly dynamic system requires reliable data concerning hydraulic parameters (Šimůnek *et al.*, 2011), preferably under actual field conditions (Angulo-Jaramillo *et al.*, 1997; Yoon *et al.*, 2007). It was hypothesized that adopting CA affects various components of the soil water balance by modifying the physical domain of the soil, thereby impacting root water uptake. A CA field experiment with a 7-year transition period was used to test the hypothesis through the simulation of soil water using Hydrus-2D. The entire crop growth period was divided into three periods, and a simulation was performed using field-measured soil and plant parameters.

MATERIALS AND METHODS

The CA experiment with rice (summer)-wheat (winter) rotation was initiated at the ICAR-Indian Agricultural Research Institute farm (28.64°N, 77.15°E, 228 m above mean sea level), New Delhi, in 2010. The climate is semi-arid, with hot, dry summer and cold winter conditions. The average annual rainfall is 710 mm, it is mainly rainy (~80%) between July and September (the southwest monsoon). The surface soil (0-20 cm) has a clay loam texture, while it is loam on the subsurface. The weather conditions in the *rabi* (winter) season (November to April) for the two observation years are given in Fig. 1.

Two treatments were selected for the study: conventional tillage (CT) (transplanted rice followed by conventionally tilled wheat) and a zero-till system for all three crops (rice-mungbean-wheat in sequence) (conservation agriculture or CA thereafter). Rice was direct-seeded during the rainy season, wheat in the winter, and mungbean was grown in the summer. All mungbean residues and 40% of the rice and wheat residues were retained as mulch during subsequent crops. In CT, two disking and two harrowings (~15 cm soil depth) were performed in rice, followed by levelling with a wooden plank. The seed rates of rice (var. PRH-10), wheat (var. HDCSW-18), and mungbean (var. SML-668) were 20, 100, and 20 kg seed ha⁻¹, respectively, with 20 cm row-to-row spacing. Approximately 2 cm of standing water was maintained in CT (mainly every fourth day), and irrigation maintained for the most part at 50% soil moisture depletion was applied in CA in rice. The wheat crop was irrigated at five critical stages in CA and CT, on each occasion with ~6 cm irrigation. The critical stages were crown root

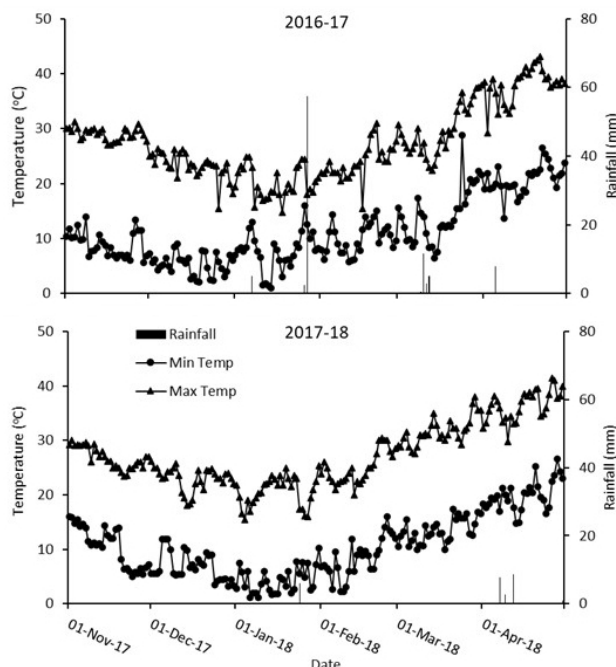


Fig. 1. Daily meteorological data covering the entire wheat growth season (2016-17 and 2017-18).

initiation (CRI, 20-25 days after sowing; DAS), tillering (40-45 DAS), active vegetative (60-65 DAS), panicle initiation (80-85 DAS) and grain filling (100-105 DAS) in wheat. The rice and wheat crops were given uniform applications of 120:60:40 kg ha⁻¹ of N, P₂O₅, and K₂O, respectively. Half of the N and the total dose of P₂O₅ and K₂O were applied as basal fertilizers during sowing. The remaining half dose of N was applied as top-dressing through the application of urea in two equal portions at 30 and 50 days after the rice was sown, while for the wheat crop, the remaining half of the nitrogen was applied as a top-dressing after the first irrigation at the CRI stage. The basal dose of the nutrients was provided through the application of di-ammonium phosphate, urea, and muriate of potash. The weeds were controlled by applying a pre-emergence spray of pendimethalin (1.0 kg a.i. ha⁻¹) and a post-emergence spray of bispyribac (25 g a.i. ha⁻¹) at 20 DAS. A tank-mix solution of isoproturon (1 kg a.i. ha⁻¹) and 2,4-D sodium salt (0.5 kg a.i. ha⁻¹) was applied at 35 DAS to control the grassy and broadleaf weeds in the wheat crop.

Undisturbed soil cores (8 replications) were collected from 0-15, 15-30, 30-45, and 45-60 cm soil layers after the harvest of the wheat crop in the 6th and 7th years of the experiment. Additionally, core samples were taken on 34, 103 DAS in 2016-17 when wheat was grown to monitor the early- and mid-season variations in soil bulk density (BD). The samples were saturated through capillarity, and the saturation water contents (θ_s) were recorded. The field-saturated hydraulic conductivity (K_s) was determined at the 0-15, 15-30, and 30-45, and also at the 45-60 cm soil layer using the Guelph Permeameter (GP; Model 2800K1,

Soil Moisture Equipment Corporation, Santa Barbara). The GP is a constant head well permeameter (Reynolds *et al.*, 2002), consisting of a Marriott bottle arrangement to maintain a constant water level inside the hole at the soil layers mentioned above. The steady-state water entry into the soil from the hole was measured.

The soil water content in the 0-15 cm layer was monitored gravimetrically (and converted to volume wetness using the BD values of the respective layers). A neutron moisture probe (CPN-503 DR Hydroprobe, Campbell Pacific Nuclear International Inc., USA) was used for other layers *viz.*, 15-30, 30-45, and 45-60 cm.

The leaf area index was measured using a plant canopy analyser (LAI-2000, LI-COR, Lincoln, NE, USA), and the fraction of the intercepted photosynthetically active radiation (fIPAR) was determined by using a line quantum sensor (LI-COR). Both measurements were taken on clear days between 11:30 and 12:30 (Saha *et al.*, 2015).

The roots were sampled from multiple numbers of plants in a plot (5-7, depending on the crop growth stage) at the grain filling stage. Each plant was cut above ground, and the roots were collected using a root auger (Ahmad *et al.*, 2018). The roots were washed and scanned through the use of a root-scanner (LA-1600; Win-RHIZO software, Regent Instruments Inc., Canada) in order to record their morphological characteristics (length, surface area, volume, and average diameter). Post-scanning, the roots were oven-dried at 65°C to constant weights, and the dry weights were recorded. All root parameters were divided by the volume of the core in order to obtain the respective densities for each soil layer.

Hydrus-2D (Šimůnek *et al.*, 2011) numerically solves the Richards equation (Richards, 1931) for the flow of water through soil, as given below:

$$\frac{\partial \theta}{\partial t} = \frac{\partial}{\partial x} \left[K \frac{\partial \Psi}{\partial x} \right] + \frac{\partial}{\partial z} \left[K \frac{\partial \Psi}{\partial z} \right] + \frac{\partial K}{\partial z} + S, \quad (1)$$

where: θ is the soil water content, ψ is the soil matric potential, and K is the unsaturated hydraulic conductivity. It is a function of θ , and S is the sink term (details below), computed using the Feddes model (Feddes *et al.*, 1978).

In the present study, the measured θ_s and K_s values were given as inputs to derive the ' α ' and ' n ' parameters of the van Genuchten model (van Genuchten, 1980) through inverse modelling. The residual water content (θ_r) was assumed at the wilting point. The effective soil water content (Se) and unsaturated hydraulic conductivity [$K(\theta)$] were computed as shown below for the numerical simulation of daily soil water contents.

$$Se = \frac{\theta - \theta_r}{\theta_s - \theta_r}, \quad (2)$$

$$Se = \left[\frac{1}{1 + (\alpha\psi)^n} \right]^m, \quad (3)$$

$$K(\theta) = K_s Se_e^1 \left[1 - \left(1 - Se_e^{\frac{1}{m}} \right)^2 \right]. \quad (4)$$

Parameter m is related to the soil pore size and is equal to $1-1/n$.

Root water uptake (S , the sink term) was computed using the Feddes model (Feddes *et al.*, 1978).

$$S(\psi, x, z) = \alpha(\psi, x, z) b(x, z) T_p L, \quad (5)$$

where: $\alpha(\psi, x, z)$, a water-stress response function (SRF), is a dimensionless function of the soil matric suction (ψ); $b(x, z)$ is the normalized water-uptake distribution function (UDF, cm^{-2}); T_p is the potential transpiration rate (cm d^{-1}), and L (cm) is the surface length associated with transpiration (width of the canopy coverage). The SRF was assumed to be 1 for $-1 > \psi > -50$ kPa for wheat at the maximum daily T_p , and again as 1 for $-1 > \psi > -200$ kPa and $-1 > \psi > -90$ kPa for the minimum daily T_p at a given simulation period. The α values decrease linearly as ψ changes from $-50/90$ to -1500 kPa for wheat. The determination of UDF requires the maximum rooting depth, the depth of the maximum root intensity, the maximum rooting radius (horizontally from the base of the plant), and the radius of maximum root intensity (average radius, cm) as inputs (Table 1). The full depth and the maximum horizontal spread were taken at root length density (RLD) $> 0.1 \text{ cm cm}^{-3}$, while the depth of the maximum rooting intensity was considered at RLD $> 0.75 \text{ cm cm}^{-3}$. The L values ranged between 18-22 cm across the simulation periods and treatments. T_p was equal to the maximum root water uptake under a non-limiting soil water regime. Similarly, the potential evaporation rate (Ep) was the complete possible soil evaporation rate in the case of water availability being non-limiting. These components were functions of evapotranspiration (ET_c), LAI, and fIPAR.

Table 1. Wheat root parameters as input to Hydrus-2D (CA and CT stand for conservation agriculture and conventional tillage, respectively)

Root parameter (cm)	Period I		Period II		Period III	
	CA	CT	CA	CT	CA	CT
Maximum rooting depth	45	45	60	60	60	60
Depth of maximum root intensity	15	15	15	15	15	15
Maximum rooting radius	9	9	11	11	11	11

The FAO Penman-Monteith method was used for daily reference evapotranspiration (ET_0) computation from daily weather parameters recorded in the agromet observatory adjacent to the experimental plots (Allen *et al.*, 1998). The ET_c (crop stage-wise) was obtained by multiplying ET_0 by the crop coefficient (K_c).

The ET_c was partitioned into Ep by using the following formula (Ritchie, 1972) and T_p from the difference:

$$Ep = ETc \exp(-k LAI) , \quad (6)$$

where: k is the radiation extinction coefficient computed from the relationship between fIPAR and LAI (Saha *et al.*, 2015).

The simulation was performed for three different growth periods: initial (Period I, 26-52 and 43-71 DAS in the 1st and 2nd years, respectively), intermediate (Period II, 52-92, and 71-100 DAS), and final (Period III, 92-120 and 100-131 DAS). The upper boundary of the soil domain was set at the atmospheric boundary, and the lower one was the free drainage. The vertical sides of the domain were considered to be the no-flux boundaries. There were three time-variable boundary conditions. Two were calculated from the weather variables (max and min temperature, relative humidity, wind speed, and sunshine hours) and plant parameters (fIPAR and crop coefficient to compute the Ep and the Tp). The third time-variable boundary condition was the amount of rainfall (Fig. 2). Daily values were used for the simulation.

After successful validation, the field water balance components (changes in soil water, actual transpiration and evaporation rates, and drainage from the soil profile) for both years were obtained as model outputs.

Data were subjected to an analysis of variance following randomized block design using the Statistical Analysis System (SAS, 2006) available at the Indian NARS Statistical Computing Portal (<http://stat.iasri.res.in/sscnarsportal>). The means were subjected to a significant difference at $p < 0.05$ using Tukey's HSD test. MS Excel was used for the basic calculation, interpretation, and preparation of the figures.

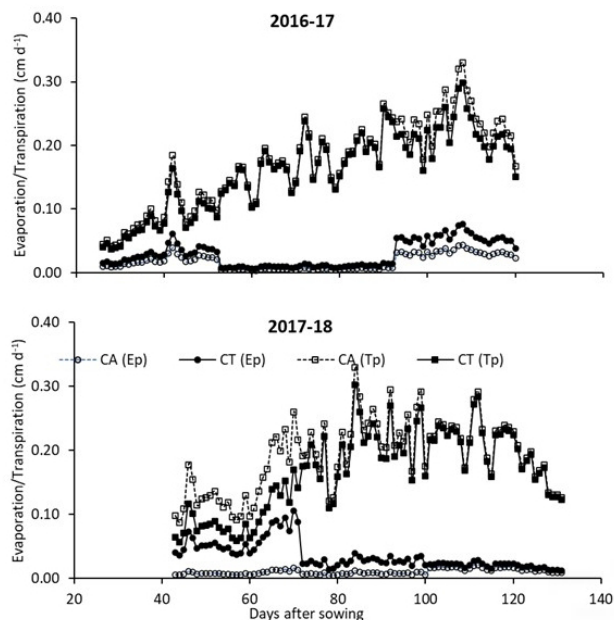


Fig. 2. Potential evaporation (Ep) and transpiration (Tp) in wheat during 2016-17 and 2017-18 under conservation agriculture (CA) and conventional tillage (CT) practices.

RESULTS

The soil water content (average of 0-60 cm) was higher in CA for most growing periods (Fig. 3). The simulated results agreed with the field-measured soil water content values [$R^2 = 0.76$ and 0.80 for CA and CT, respectively; $p < 0.01$]. RMSE and nRMSE were 1.1 and 5.2 in CA and 1.1 and 3.6 in CT. The initial period of the simulation showed a higher soil water content under CA than CT. A similar trend was also observed in the later phase.

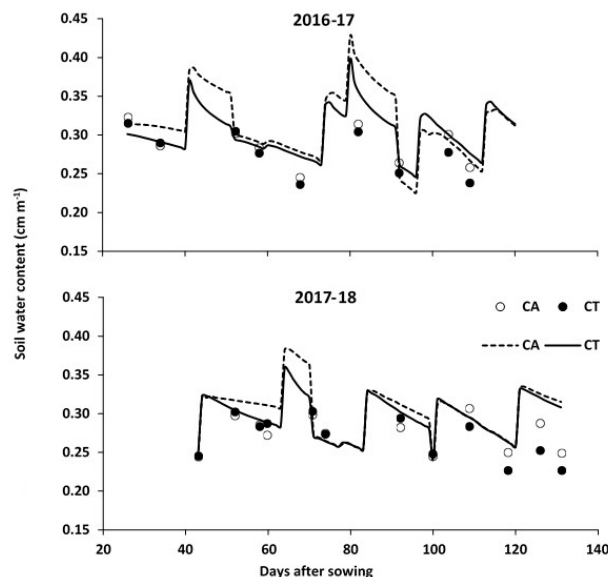


Fig. 3. Simulated (lines) and measured (points) of soil water content changes in wheat during the year 2016-17 and 2017-18 (CA and CT refer to conservation agriculture and conventional tillage, respectively).

Table 2. Soil hydraulic properties as input parameters to Hydrus-2D

Treatment	Simulation period	Soil layer (cm)	θ_r (cm^3)	θ_s (cm^{-3})	K_s (cm d^{-1})	BD (g cm^{-3})
CA	Period I and II	0-15	0.085	0.42	6.8	1.67
		15-30	0.072	0.43	5.9	1.78
		30-45	0.079	0.39	6.4	1.81
CT	Period I and II	0-15	0.082	0.41	26.7	1.63
		15-30	0.070	0.36	21.2	1.80
		30-45	0.075	0.42	18.3	1.83
CA	Period III	0-15	0.085	0.43	7.3	1.70
		15-30	0.075	0.41	6.1	1.87
		30-45	0.070	0.41	7.2	1.83
CT	Period III	0-15	0.079	0.42	27.8	1.78
		15-30	0.080	0.39	22.4	1.89
		30-45	0.075	0.41	19.6	1.84

θ_r , θ_s , α , and n are van Genuchten parameters; K_s : saturated hydraulic conductivity, BD: bulk density; CA and CT stand for conservation agriculture and conventional tillage, respectively.

The effect of tillage practices on the saturated soil water content (θ_s) was similar at all depths (Table 2). The saturated hydraulic conductivity (K_s) was substantially higher under CT in all the layers. The K_s values decreased down the profile under CT; however, it was marginally lower at 15-30 cm compared to the 0-15 and 30-45 cm layers in CA.

The fIPAR and LAI confirmed the differential micro-meteorological growing conditions under CA and CT practices. LAI differed between the CA and CT practices in both years, especially in the intermediate and later stages (Table 3). It was 26-38% higher ($p < 0.01$) under CA in the first year, while in the next year, LAI under CA was more than twice that under CT. The fIPAR was higher for CA at all the measurement periods. It was 13, 3, and 11% higher ($p < 0.05$) at 47, 78, and 112 DAS (year 1), and 83% ($p < 0.05$) and 33% ($p < 0.01$) higher for CA at 61 and 72 DAS (year 2), respectively. Linear models, with similar slopes for CA and CT, satisfactorily explained the LAI and $\ln(1-fIPAR)$ relationship.

The effect of CA on root growth was evident (Fig. 4). In the surface layer (0-15 cm), RLD was 20% higher ($p < 0.05$) under CA, while in the 15-30 cm layer, it was twice that under CT. CA resulted in a higher root surface area density in the 15-30 cm layer, while the root weight density was

Table 3. Leaf area index, a fraction of intercepted photosynthetically active radiation at different growth stages in the year 2016-17 and 2017-18 under the conservation agriculture (CA) and conventional tillage (CT) practices

Year	Days after sowing	CA	CT
Leaf area index (LAI)			
2016-17	57	1.88a±0.10	1.55a±0.12
	68	4.09a±0.12	3.26b±0.18
	84	3.83a±0.16	2.77b±0.09
2017-18	61	3.77a±0.14	1.13b±0.06
	72	4.27a±0.12	1.61b±0.08
	84	4.46a±0.07	2.54b±0.05
	97	4.87a±0.15	3.41b±0.10
	130	3.57a±0.09	2.82b±0.06
Fraction of intercepted photosynthetically active radiation (fIPAR)			
2016-17	47	0.82a±0.01	0.73b±0.04
	78	0.97a±0.00	0.94b±0.01
	112	0.88a±0.02	0.80b±0.03
2017-18	61	0.95a±0.00	0.52b±0.03
	72	0.97a±0.00	0.73b±0.02
Extinction coefficient		-0.75	-0.85

Mean values followed by different small letters in a row are significantly different at $p < 0.05$.

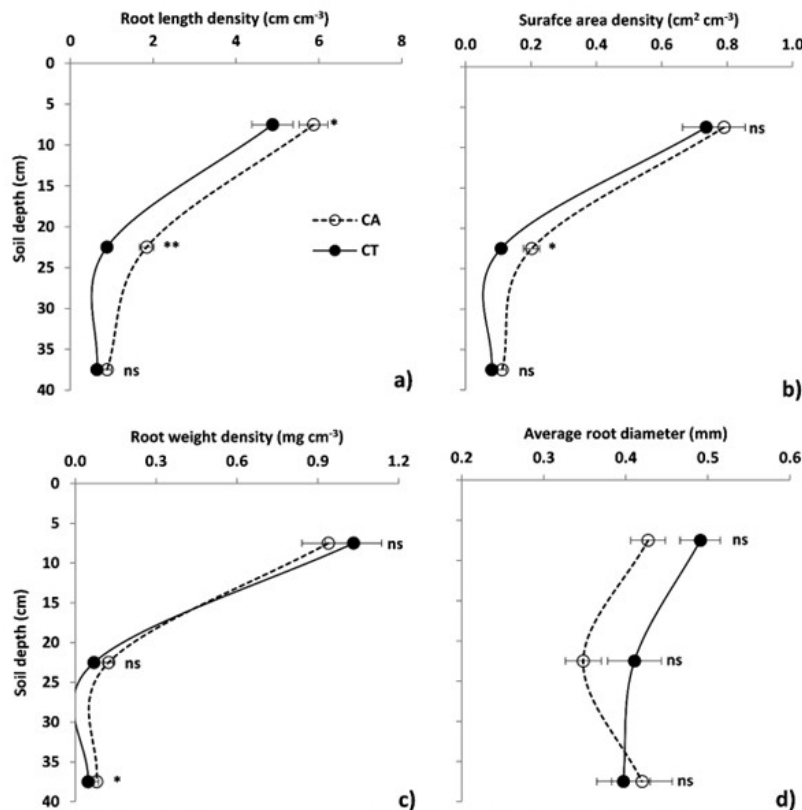
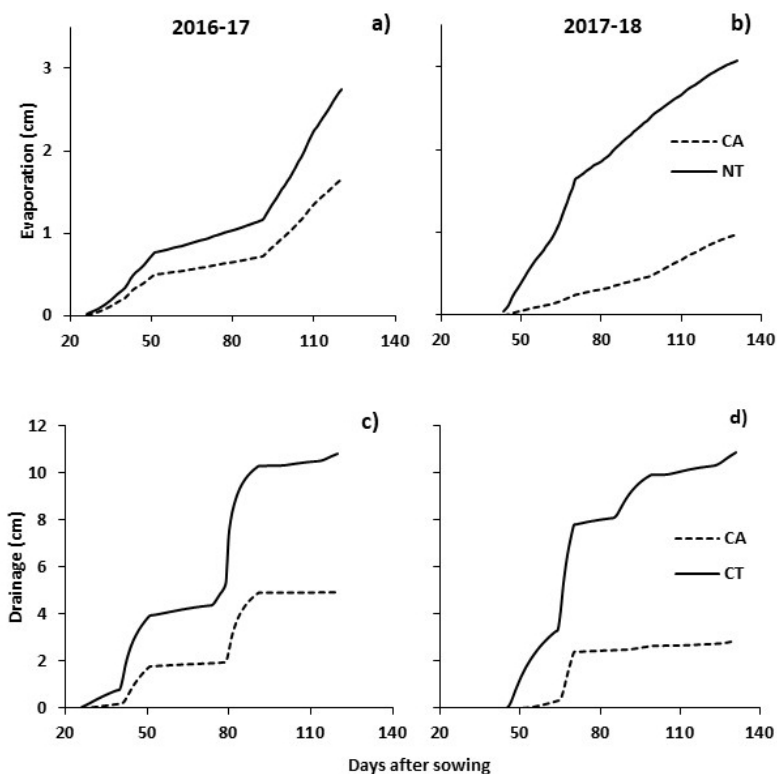


Fig. 4. The root morphological parameters of wheat in the 0-15, 15-30, and 30-45 cm soil layers (mean of 2016-17 and 2017-18), a – root length density, b – surface area density, c – root weight density, d – average root diameter, the ± standard error of the mean is given as horizontal bars, at: * $p < 0.05$ and ns – non-significance, respectively.

Table 4. Simulated soil water balance components in different growing periods of wheat under conservation agriculture (CA) and conventional tillage (CT) practices

Period	Input								Output								Balance	
	R+I	Initial SWC		Total input		Evaporation		Drainage		Final SWC		RWU		Total output		CA	CT	
		CA	CT	CA	CT	CA	CT	CA	CT	CA	CT	CA	CT	CA	CT			
2016-17																		
I	6.0	23.7	22.6	29.7	28.6	0.51	0.77	1.8	3.9	26.2	23.0	1.1	0.8	29.6	28.5	0.1	0.1	
II	12.5	22.6	22.1	35.1	34.6	0.25	0.45	3.1	6.3	25.7	22.7	5.8	5.1	34.8	34.5	0.2	0.1	
III	12.1	18.3	19.6	30.4	31.7	0.89	1.53	0.0	0.5	22.9	23.4	6.6	6.0	30.5	31.4	-0.1	0.2	
Total	30.5	64.6	64.3	95.1	94.9	1.65	2.75	5.0	10.8	74.8	69.1	13.6	11.9	94.9	94.5	0.2	0.4	
2017-18																		
I	12.0	18.3	18.4	30.3	30.4	0.26	1.66	1.2	3.9	27.0	23.7	1.9	1.1	30.4	30.3	-0.1	0.1	
II	6.6	20.6	20.5	27.2	27.1	0.25	0.78	0.1	1.0	21.8	20.9	5.3	4.4	27.5	27.1	-0.3	0.0	
III	12.0	18.4	18.6	30.4	30.6	0.47	0.63	0.1	0.5	23.6	23.1	6.3	6.2	30.5	30.4	-0.2	0.2	
Total	30.6	57.3	57.5	87.9	88.1	0.97	3.07	1.4	5.4	72.4	67.7	13.6	11.6	88.4	87.8	-0.5	0.3	

R+I, SWC, and RWU refer to rainfall + irrigation, soil water content, and root water uptake; all values are in cm.

**Fig. 5.** Simulated daily cumulative evaporation (a and b) and drainage (c and d) in wheat during 2016-17 and 2017-18 under conservation agriculture (CA) and conventional tillage (CT) practice.

higher (67%; $p < 0.05$) in the 30-45 cm layer. The average root diameter was marginally larger under CT than it was under CA, at up to a 30 cm soil depth.

With the exception of the surface length, the root input parameters were primarily similar between CA and CT. The maximum rooting depth was 45 cm in Period I and 60 cm in Periods II and III (Table 1). Irrespective of the simulation period, the depth of the maximum root intensity was

0-15 cm, it decreased sharply beyond this layer. The horizontal spread of the roots was 9 cm (Period I) and 11 cm (Periods II and III), with the horizontal distance of maximum root intensity occurring at 3, 4, and 5 cm during the three periods. The surface length (L) varied, and CA had an average value of 10 cm as compared to 8 cm under CT during Period I, 18 vs. 16 cm in Period II, and 22 cm under CA and CT in Period III.

In the first year, a 53% higher Tp was recorded under CA than CT in Period I, which was reduced to 9% in Period II and 3% in Period III (Fig. 5). A 52-80% higher Tp was recorded under CA over the three periods in the following year. On the contrary, Ep was higher under CT as compared to CA. The difference was most evident in later stages.

In 2016-17, in simulation Period I (26-52 DAS), the cumulative evaporation was 0.77 cm under CT as compared to 0.51 cm under CA (Table 4). In Period II, 104 and 73% reductions were recorded under CA and CT, respectively. In the final simulation period (Period III, 92-120), cumulative evaporation reached its maximum value (0.89-1.53 cm). In 2017-18, there was a significant difference in initial cumulative evaporation between CT (1.66 cm) and CA (0.26 cm), which was reduced in Periods II and III.

In 2016-17, the drainage was 3.95 cm under CT as compared to 1.80 cm under CA in Period I (Table 4). It was even greater under CT in the following year, with 3.91 cm of water being lost through drainage as compared to only 1.20 cm under CA. In simulation Period II, the amount of drainage was 6.34 cm under CT as compared to 3.13 cm under CA in the first year but it varied between 0.13-1.05 cm in the second year with a marginal difference occurring between CA and CT. In the final simulation period (Period III), the drainage loss varied between 0.02-0.52

and 0.11-0.48 cm during the first and second years. The total drainage under CT was 2.2 and 3.9 times higher than under CA in the respective years of the experiment.

The daily root water uptake (RWU) increased gradually from the initial lower values to maxima which occurred during simulation Period III (Fig. 6). It was similar under CA (0.09 cm day^{-1}) and CT (0.08 cm day^{-1}) in Period I and Period II (both are 0.17 cm day^{-1}). The RWU reached a maximum value during 92-120 DAS (Period III) with 0.24 and 0.21 cm day^{-1} under CA and CT, respectively. In the following year, RWU was 55% higher under CA in Period I but was similar during Period II (0.22 and 0.20 cm day^{-1} under CA and CT, respectively), followed by a slight reduction (5%) under CA as compared to CT.

Cumulative RWU was 37% higher under CA in Period I in the first year but was similar in Period II (5.80 and 5.07 cm under CA and CT, respectively) (Table 4). The values were 6.61 and 6.00 cm under CA and CT in the final simulation period, respectively. The second year produced similar trends. Initially, it was 80% higher under CA, although the differences decreased in Period II and were marginal in Period III. The graphical representation clearly distinguished the impact of tillage on root water uptake in wheat (Fig. 7).

In the first year, the initial soil water content (SWC) was 64.6 cm under CA against 64.3 cm under CT, although the final SWC was 8% higher under CA (Table 4). The

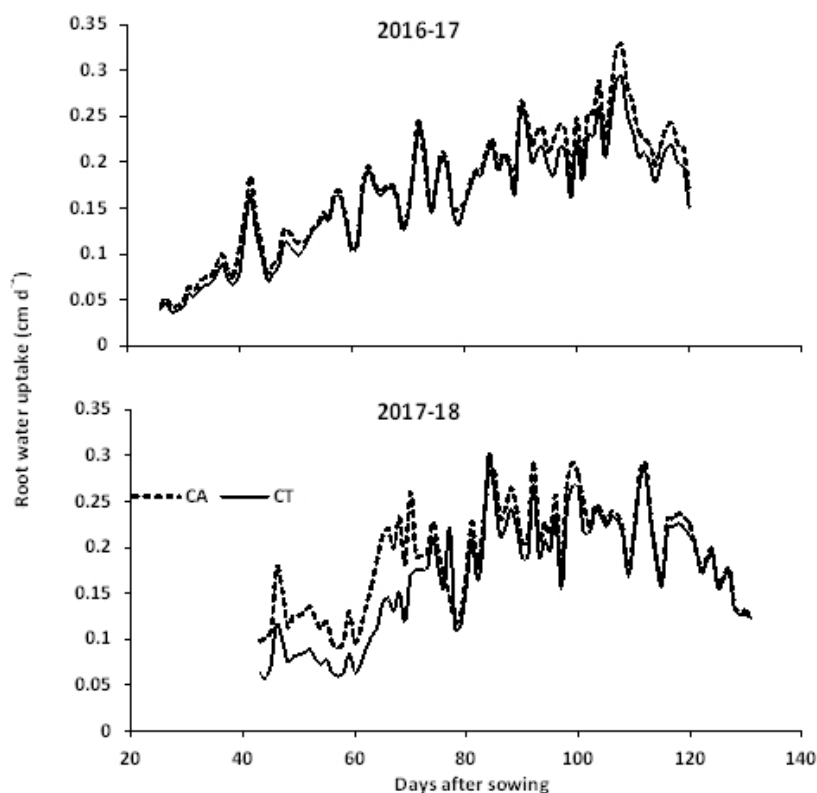


Fig. 6. Simulated daily root water uptake (RWU) in wheat during 2016-17 and 2017-18 under conservation agriculture (CA) and conventional tillage (CT) practice.

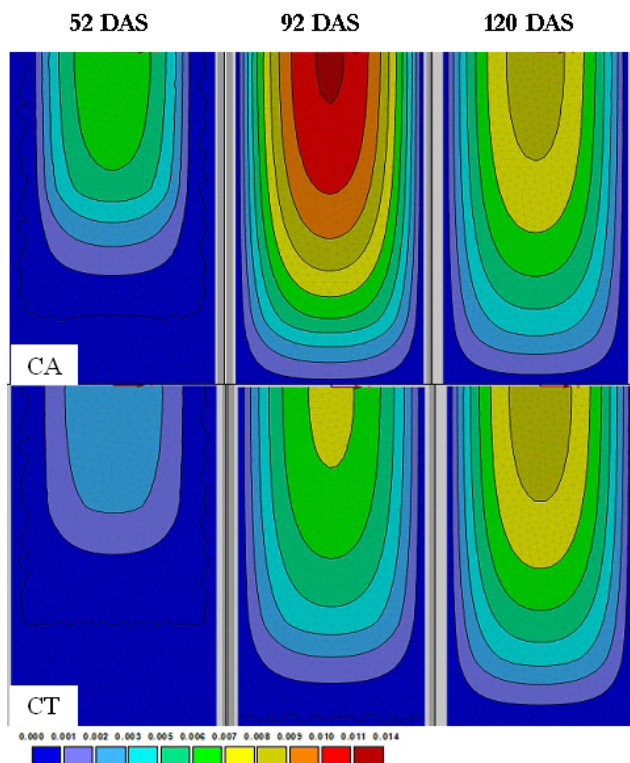


Fig. 7. Simulated average daily root water uptake (cm d^{-1}) pattern in 0-60 cm soil profile in wheat under conservation agriculture (CA) and conventional tillage (CT) practice (DAS stands for days after sowing).

evaporation loss was considerably higher (75%) under CT as compared to CA. The circumstances were similar in the case of drainage water, where the total drainage under CT was twice that under CA during the entire simulation. In contrast, RWU was higher (14%) under CA. In the second year, the initial SWC content was similar (57.3 and 57.5 cm) under CA and CT, respectively. The final SWC under CA was higher by 7%, although the evaporation and drainage losses were substantially higher, and CT was registered as producing 3- and 4-times higher evaporation and drainage, respectively, than CA. A 17% higher RWU was recorded under CA than under CT.

DISCUSSION

The change in SWC profile was aptly predicted by Hydrus-2D. The model successfully captured an increase in SWC following rain or irrigation and then a gradual decline. Differences in SWC due to tillage were apparent. Although both systems were irrigated, the higher SWC under CA was due to surface mulch preventing evaporation loss. Lower evaporation and drainage facilitated a better soil water regime under CA (*e.g.*, Mondal *et al.*, 2019b), which improved the water uptake by the crop (Liu *et al.*, 2020).

The relevant hydraulic parameters are essential for characterizing the unsaturated/vadose zone flow processes. These parameters are directly measured or estimated

from surrogate soil data like texture and bulk density. In the present study, the θ_s was determined through the capillary wetting of undisturbed soil cores to saturation but it was not taken as a proxy for porosity. θ_r was assumed to be the water content at the wilting point. Measured values of θ_s and θ_r were averaged (\pm SE) at around 0.41 (\pm 0.006) and 0.08 (\pm 0.002), respectively, with no notable differences occurring between CA and CT. The K_s values had a larger range and were higher under CT, indicating an increase in soil drainage. A relatively higher proportion of soil macropores under CT was reported earlier in the same experimental field (Mondal *et al.*, 2019b). Although the Rosetta-estimated K_s values for clay loam soil were close to the measured K_s values in the CT system, the same parameters in CA deviated from the estimated values. Therefore, the estimation of K_s through Rosetta might not be reliable, when changes in the physical conditions of the soil (as in CA) are predictable (Ahmad *et al.*, 2018). The adoption of no-tillage modified the soil hydraulic functions through changes in the pore structure, which was apparent in the K_s values. However, the ' α ' and ' n ' parameters were comparable with the class-average table values for the clay loam texture.

The potential transpiration rate (T_p) was negligible during the initial simulation due to lower LAI , which has also been reported by Aggarwal *et al.* (2017) and Ahmad *et al.* (2018) under similar agroclimatic conditions. CA produced higher LAI , especially in the second year, which was reflected appropriately in T_p . The E_p is regulated by soil surface management like tillage and crop residue mulch. CT induced a higher E_p . The difference was significant during the initial simulation when the soil exposure under CT was unlike that in CA, where the soil was residue-covered. During the final simulation period, canopy ground coverage was higher under CA (higher LAI and fractional IPAR), thereby reducing soil evaporation as compared to CT. Crop establishment was faster under CA (visual observation, data not presented), thereby facilitating better growth and more extensive canopy coverage. LAI and fIPAR were higher, even during the initial simulation period, which subdued the soil evaporation under CA. Moreover, the soil surface was covered by residues, which prevented water loss to the atmosphere. The effect of mulch on reducing soil evaporation has been widely reported (*e.g.*, Chen *et al.*, 2007, 2015; Chakraborty *et al.*, 2008), as it can reduce the irrigation water requirement of the crop. Studies from both irrigated and rainfed regions around the US reported a 10-13 cm irrigation water saving through the adoption of no-tillage practices (Pryor, 2006; Klocke *et al.*, 2009). In the present study, both of the tillage systems received similar levels of irrigation or rain, so the water-saving could not be evaluated. However, the SWC change profile indicated greater SWC under CA and provided scope for maximizing soil water use and minimizing losses.

Hydrus-2D successfully simulated the root water uptake and estimated a 14-17% higher uptake in CA, which was mainly attributed to limited drainage rather than CT. Better root growth under CA also contributed to increased water uptake by the crop. Many authors have reported improved root growth under CA which is related to the soil water regime (e.g., Lampurlanés *et al.*, 2001; Mondal *et al.*, 2019a; Mehra *et al.*, 2020). The spreading of roots in the soil can aid in predicting crop transpiration (Šimůnek *et al.*, 2011). CA improved root growth in the subsurface (>15 cm) due to the moderation of soil-air-water retention and hydrothermal regimes (Mondal *et al.*, 2019a). In a global meta-analysis, Mondal *et al.* (2020b) reported significant increases in root growth in the soil under CA, which was in agreement with a higher mean-weight diameter of aggregates and water content at field capacity. CA improves soil structural stability, which modifies pore sizes in favour of higher soil water retention. Root growth and development were meticulously monitored in terms of depth distribution and temporal changes in the present study. Given the uncertainties involved in root sampling and representing field conditions, the root water uptake was found to be in an acceptable range. The tillage effect could also be effectively portrayed. The simulation of water uptake by wheat was symmetrical in shape and centred on the primary root, matching the horizontal zone of maximum root water uptake. Root water uptake had a substantial influence over the yield of the wheat crop, which was more in favour of CA.

It may not be assumed that the changes to soil properties will be insignificant over the growing period, and also the temporal variation may affect the output of the model (Alletto *et al.*, 2015). The present study used three simulation results, these were appropriately distributed over the crop growth period and summarized for a cumulative assessment of soil water balance and crop water uptake. This produced an improved overview of the impact of tillage in modifying the soil water system, as was demonstrated previously by Ahmad *et al.* (2018). Hydrus-2D effectively simulated the soil water dynamics, thereby facilitating reliable estimates of root water uptake, which was otherwise technically challenging to measure in the field. Moreover, the model could reveal the differences due to tillage practices and relate them to crop growth and development. Overall, CA effectively modified the soil domain, especially in the subsurface zone, which led to improved root growth and increased root water uptake. Although the impact of CA on soil water retention is governed by the soil type and agroclimatic conditions, an increase in root water uptake was predicted, thereby improving canopy cover and increasing yields. A significant reduction in soil evaporation loss due to surface residue mulch and reduced drainage due to the modifications of soil pores can increase water availability and improve soil resilience to climate change.

This has more significant implications in arid and semi-arid areas where the limitation of water availability has always been a concern.

CONCLUSIONS

The following conclusions have emerged from the study.

1. Hydrus-2D successfully captured the differences in evaporation, root water uptake, and profile drainage, which for the most part favoured conservation agriculture.
2. Better crop establishment, early canopy cover, and crop residue mulch due to conservation agriculture reduced soil evaporation loss. Loss by drainage was also limited in conservation agriculture, leading to a higher rate of soil water retention.
3. With improved soil water retention, enhanced root growth facilitated a higher soil water uptake in wheat under conservation agriculture.
4. Finally, the root-zone soil water balance was successfully simulated using Hydrus-2D, this revealed a clear difference between the tillage practices. This result may be used to improve irrigation water management in the wheat crop.

ACKNOWLEDGEMENTS

The authors acknowledge the facilities, help, and support of the Heads of Divisions of Agricultural Physics and Agronomy, ICAR-IARI, during the study. The primary author acknowledges the support of the Directorate, ICAR in general, and the ICAR Research Complex, Patna for the successful completion of the study.

Conflict of interest: The Authors declare they have no conflict of interest.

REFERENCES

- Aggarwal P., Bhattacharyya R., Mishra A.K., Das T.K., Šimůnek J., Pramanik P., Sudhishri S., Vashisth A., Krishnan P., Chakraborty D., and Kamble K.H., 2017. Modelling soil water balance and root water uptake in cotton grown under different soil conservation practices in the Indo-Gangetic Plain. *Agr. Ecosyst. Environ.*, 240, 287-299, <https://doi.org/10.1016/j.agee.2017.02.028>
- Ahmad M., Chakraborty D., Aggarwal P., Bhattacharyya R., and Singh R., 2018. Modelling soil water dynamics and crop water use in a soybean-wheat rotation under chisel tillage in a sandy clay loam soil. *Geoderma*, 327, 13-24, <https://doi.org/10.1016/j.geoderma.2018.04.014>
- Allen R.G., Pereira L.S., Raes D., and Smith M., 1998. Crop evapotranspiration-Guidelines for computing crop water requirements - FAO Irrigation and drainage paper 56. Fao, Rome, 300(9), D05109.
- Alletto L., Pot V., Giuliano S., Costes M., Perdrieux F., and Justes E., 2015. Temporal variation in soil physical properties improves the water dynamics modeling in a conventionally-tilled soil. *Geoderma*, 243, 18-28, <https://doi.org/10.1016/j.geoderma.2014.12.006>

- Angulo-Jaramillo R., Thony J.L., Vachaud G., Moreno F., Fernandez-Boy E., Cayuela J.A., and Clothier B.E., 1997.** Seasonal variation of hydraulic properties of soils measured using a tension disk infiltrometer. *Soil Sci. Soc. Am. J.*, 61, 27-32, <https://doi.org/10.2136/sssaj1997.03615995006100010005x>
- Chakraborty D., Nagarajan S., Aggarwal P., Gupta V.K., Tomar R.K., Garg R.N., Sahoo R.N., Sarkar A., Chopra U.K., Sarma K.S.S., and Kalra N., 2008.** Effect of mulching on soil and plant water status, and the growth and yield of wheat (*Triticum aestivum* L.) in a semi-arid environment. *Agr. Water Manage.*, 95, 1323-1334, <https://doi.org/10.1016/j.agwat.2008.06.001>
- Chen S.Y., Zhang X.Y., Pei D., Sun H.Y., and Chen S.L., 2007.** Effects of straw mulching on soil temperature, evaporation and yield of winter wheat: field experiments on the North China Plain. *Ann. Appl. Biol.*, 150, 261-268, <https://doi.org/10.1111/j.1744-7348.2007.00144.x>
- Chen Y., Liu T., Tian X., Wang X., Li M., Wang S., and Wang Z., 2015.** Effects of plastic film combined with straw mulch on grain yield and water use efficiency of winter wheat in Loess Plateau. *Field Crop Res.*, 172, 53-58, <https://doi.org/10.1016/j.fcr.2014.11.016>
- Das B., Chakraborty D., Singh V.K., Ahmed M., Singh A.K., and Barman A., 2016.** Evaluating fertilization effects on soil physical properties using a soil quality index in an intensive rice-wheat cropping system. *Pedosphere*, 26, 887-894, [https://doi.org/10.1016/S1002-0160\(15\)60093-5](https://doi.org/10.1016/S1002-0160(15)60093-5)
- FAO, 2015.** Status of the world's soil resources (SWSR)-main report. Food and Agriculture Organization of the United Nations and Intergovernmental Technical Panel on Soils, Rome, Italy 650.
- Feddes R.A., Kowalik P.J., and Zaradny H., 1978.** Simulation of field water use and crop yield. Pudoc, Wageningen. Simulation Monographs.
- Jat M.L., Chakraborty D., Ladha J.K., Rana D.S., Gathala M.K., McDonald A., and Gerard B., 2020.** Conservation agriculture for sustainable intensification in South Asia. *Nature Sustainability*, 3, 336-343, <https://doi.org/10.1038/s41893-020-0500-2>
- Jatav R.A., Roy D.E., Kumar V.I., Thomas P.A., Mondal S., Yadav R.A., and Chakraborty D., 2018.** Conservation agriculture impact on soil hydro-physical properties in maize-wheat rotation. *J. Agr. Physics.*, 2, 168-72.
- Klocke N.L., Currie R.S., and Aiken R.M., 2009.** Soil water evaporation and crop residues. *Trans. ASABE*, 52, 103-110, <https://doi.org/10.13031/2013.25951>
- Kukul S.S. and Aggarwal G.C., 2003.** Puddling depth and intensity effects in rice-wheat system on a sandy loam soil: I. Development of subsurface compaction. *Soil Till. Res.*, 72, 1-8, [https://doi.org/10.1016/S0167-1987\(03\)00093-X](https://doi.org/10.1016/S0167-1987(03)00093-X)
- Lampurlanés J., Angás P., and Cantero-Martínez C., 2001.** Root growth, soil water content and yield of barley under different tillage systems on two soils in semiarid conditions. *Field Crop Res.*, 69, 27-40, [https://doi.org/10.1016/S0378-4290\(00\)00130-1](https://doi.org/10.1016/S0378-4290(00)00130-1)
- Liu Z., Ma F.Y., Hu T.X., Zhao K.G., Gao T.P., Zhao H.X., and Ning T.Y., 2020.** Using stable isotopes to quantify water uptake from different soil layers and water use efficiency of wheat under long-term tillage and straw return practices. *Agr. Water Manage.*, 229, 105933, <https://doi.org/10.1016/j.agwat.2019.105933>
- Mehra P., Kumar P., Bolan N., Desbiolles J., Orgill S., and Denton M.D., 2020.** Changes in soil-pores and wheat root geometry due to strategic tillage in a no-tillage cropping system. *Soil Res.*, 59, 83-96, <https://doi.org/10.1071/SR20010>
- Mondal S., Chakraborty D., Das T.K., Shrivastava M., Mishra A.K., Bandyopadhyay K.K., Aggarwal P., and Chaudhari S.K., 2019a.** Conservation Agriculture had a Strong Impact on the Sub-Surface Soil Strength and Root Growth in Wheat after a 7-year Transition Period. *Soil Till. Res.*, 195, 104385, <https://doi.org/10.1016/j.still.2019.104385>
- Mondal S., Das T.K., Thomas P., Mishra A.K., Bandyopadhyay K.K., Aggarwal P., and Chakraborty D., 2019b.** Effect of conservation agriculture on soil hydro-physical properties, total and particulate organic carbon and root morphology in wheat (*Triticum aestivum*) under rice (*Oryza sativa*)-wheat system. *Indian J. Agr. Sci.*, 89, 46-55, <https://doi.org/10.56093/ijas.v89i1.86126>
- Mondal S., Poonia S.P., Mishra J.S., Bhatt B.P., Karnena K.R., Saurabh K., Kumar R., and Chakraborty D., 2020a.** Short-term (5 years) impact of conservation agriculture on soil physical properties and organic carbon in a rice-wheat rotation in the Indo-Gangetic plains of Bihar. *Eur. J. Soil Sci.*, 71(6), 1076-1089, <https://doi.org/10.1111/ejss.12879>
- Mondal S., Chakraborty D., Bandyopadhyay K.K., Aggarwal P., and Rana D.S., 2020b.** A global analysis of the impact of zero-tillage on soil physical condition, organic carbon content, and plant root response. *Land Degrad. Develop.*, 31, 557-567, <https://doi.org/10.1002/ldr.3470>
- Pryor R., 2006.** Switching to no-till can save irrigation water. Univ. Nebraska-Lincoln Ext. Pub. EC196-3. Available at <http://ianrpubs.unl.edu/epublic/live/ec196/build/ec196-3.pdf> (Original not seen).
- Reynolds W.D., Elrick D.E., Youngs E.G., Amoozegar A., Booltink H.W.G., and Bouma J., 2002.** Saturated and field-saturated water flow parameters. In: *Methods of Soil Analysis, Part 4. Physical Methods* (Eds J. Dane, C. Topp), 797-878. SSSA, Madison, WI.
- Richards L.A., 1931.** Capillary conduction of liquids through porous mediums. *Physics*, 1, 318-333, <https://doi.org/10.1063/1.1745010>
- Ritchie J.T., 1972.** Model for predicting evaporation from a row crop with incomplete cover. *Water Resour. Res.*, 8, 1204-1213, <https://doi.org/10.1029/WR008i005p01204>
- Roger-Estrade J., Richard G., Dexter A.R., Boizard H., De Tourdonnet S., Bertrand M., and Caneill J., 2009.** Integration of soil structure variations with time and space into models for crop management. A review. *Agron Sustain Dev.*, 29, 135-142, <https://doi.org/10.1051/agro:2008052>
- SAS Institute Inc., 2006.** Online doc. 9.1.3. Cary, NC, USA. <http://support.sas.com/onlinedoc/913/docMainpage.jsp>
- Saha S., Sehgal V.K., Chakraborty D., and Pal M., 2015.** Atmospheric carbon dioxide enrichment induced modifications in canopy radiation utilization, growth and yield of chickpea (*Cicer arietinum* L.). *Agr. Forest Meteorol.*, 202, 102-111, <https://doi.org/10.1016/j.agrformet.2014.12.004>
- Šimůnek J., van Genuchten M.T., and Šejna M., 2008.** Development and applications of the HYDRUS and STANMOD software packages and related codes. *Vadose Zone J.*, 7, 587-600, <https://doi.org/10.2136/vzj2007.0077>

- Šimůnek J., van Genuchten M.T., and Šejna M., 2011.** The HYDRUS software package for simulating two- and three-dimensional movement of water, heat, and multiple solutes in variably-saturated media, Technical Manual version 2.0, PC-Progress, Prague, Czech Republic.
- van Genuchten M.T., 1980.** A closed-form equation for predicting the hydraulic conductivity of unsaturated soils 1. *Soil Sci. Soc. Am. J.*, 44, 892-898, <https://doi.org/10.2136/sssaj1980.03615995004400050002x>
- Whalley W.R., Watts C.W., Gregory A.S., Mooney S.J., Clark L.J., and Whitmore A.P., 2008.** The effect of soil strength on the yield of wheat. *Plant Soil*, 306, 237-247, <https://doi.org/10.1007/s11104-008-9577-5>
- Yoon Y., Kim J.G., and Hyun S., 2007.** Estimating soil water retention in a selected range of soil pores using tension disc infiltrometer data. *Soil Till. Res.*, 97, 107-116, <https://doi.org/10.1016/j.still.2007.09.003>